Struct Multidisc Optim (2006) 32: 161–167
DOI 10.1007/s00158-005-0577-2

INDUSTRIAL APPLICATIONS

Dong-chan Lee · Hyeun-seok Choi · Chang-soo Han

Design of automotive body structure using multicriteria optimization

Received: 21 June 2005 / Revised manuscript received: 18 August 2005 / Published online: 9 June 2006

Abstract Considerable effort has been invested into improving the performance of mechanical structures comprised of multiple substructures. Most mechanical structures are complex and are essentially multicriteria optimization problems with objective functions retained as constraints. The weight of each factor can be defined according to the effects of and the priorities among objective functions, and a single Pareto-optimal solution exists for the criteria-defined constraints. In this paper, a multicriteria optimization design based on the Pareto-optimal sensitivity is applied to the noise, vibration, and harshness qualities of automotive bodies.

Keywords Multicriteria · Pareto optimum solution · Idle shake · Wheel unbalance shake · Road shake · MAC (modal assurance criteria)

Notation

X	Design variable set
$F(X)$	Weighted objective function
w_i	Weighting factor of i-th objective function
$L(\cdot)$	Lagrange function
S	Search direction vector
λ	Lagrange multipliers of constraints
μ	Lagrange multipliers of normalized search direction constraint
ϕ	Eigenvector

Dong-chan Lee · Hyeun-seok Choi
Department of Precision Mechanical Engineering,
Hanyang University,
Sa-1 dong, Sangnok-gu, Ansan,
Kyeonggi-do, 425-791, South Korea

Dong-chan Lee
SPACE solution Co., LTD.,
#1809, Aju BLD. 679-5,
Yeoksam-dong, Gangnam-gu,
Seoul, 135-080, Korea

Chang-soo Han (✉)
Department of Mechanical Engineering,
Hanyang University,
Sa-1 dong, Sangnok-gu, Ansan,
Kyeonggi-do, 425-791, South Korea
Tel.: +82-31-4155255
Fax: +82-31-4066242
e-mail: cshan@hanyang.ac.kr

1 Introduction

Structural designs are generally subject to both performance requirements, like strength and stiffness, and to cost constraints. Thus, it is important for a concept design to account for a minimum weight structure with maximum or optimum performance, given a set of constraints. This is why optimization techniques are essential design tools. Structural optimization can be categorized into three types: size optimization, in which the physical dimensions, such as cross-section, of the structure are used as design variables; shape optimization, where the geometric boundary of the structure is varied to obtain the optimal shape by parameterizing the structure's geometry (Bendsoe 1989; Bendsoe and Kikuchi 1988); and topology optimization, which is concerned with finding the preliminary structural configuration that meets a predefined criteria (Bendsoe and Kikuchi 1988; Bendsoe et al. 1994; Devaraj et al. 2005). These types of optimization are based on the assumption that the geometry of the structure is defined by its boundaries, and that an optimal design can be found by varying the design variables. For these reasons, optimization techniques with respect to various criteria are becoming increasingly important for the development of good initial designs. Most structural problems can be broken down into a series of related but independently definable parts based on logical decompositions, without having to define structures or substructures (the distinction between which may be ambiguous in some systems). Given sets of specifications and constraints, as well as at least one concept for a mechanical structure, the idealized design can quickly proceed to the preliminary design phase. Therefore, in structural designs, multicriteria optimization problems are often formulated such that several individual optimization methods are used not only for the weighted objective functions but also for constraints. In practical applications, there are also interactions among different criteria and objective functions. Thus, a Pareto-optimal solution is needed.

Considerable research evaluating the design of automotive body structure has been undertaken, and this will likely continue to improve design efficiency (Ding 1986; Heo and Ehmann 1991; Huizinga et al. 1997; Lee 2004; Lee and Lee 2003; Nakagawa et al. 2004).

This paper presents a multicriteria optimization design based on a Pareto-optimal sensitivity for large-scale automotive body design problems (Nishigaki and Kikuchi 2004; Raasch 2004; Rao 1996; Tsurumi et al. 2004). This method involves the interactive search directions, the relationship between design variables and objective functions, and the identification of active constraints on the gradient projection method. In the iterative process, complementary S/W tools are used.

2 Formulation of multicriterion optimization problem

Mathematically, the objective and constraint functions of a given problem are separable in the design variables x_i so that the inequality-constrained problem can be stated as.

$$\text{Find } X = \{x_1 x_2 ... x_m\}^{\mathrm{T}} \text{ which minimizes } F(X) = \sum_{i=1}^{n} f_i(X) \tag{1}$$

$$\text{subject to } g_j(X) \le 0, \quad j = 1, ..., k \tag{2}$$

For solving a sequence of problems, a weighting method is needed in which the objective is defined by a linear combination of all objective functions with nonnegative weighting factors. Thus, the objective function, $F(X)$, can be redefined by:

$$F(X) = \sum_{i=1}^{n} w_i f_i(X) \tag{3}$$

where the weighting factors w_i are normalized so that $\sum_{i=1}^{n} w_i = 1$.

This problem can be solved by the method of Lagrange multipliers; we can construct the Lagrange function L as:

$$L(X, \lambda, w) = \sum_{i=1}^{n} w_i f_i(X) + \sum_{j=1}^{k} \lambda_j g_j(X) \tag{4}$$

where $\lambda = \{\lambda_1 \lambda_2 ... \lambda_k\}^{\mathrm{T}}$ is the vector of the Lagrange multipliers.

The stationary points of the Lagrange function can be found by solving the following equations from the Kuhn–Tucker optimality condition:

$$\frac{\partial L(X, \lambda, w)}{\partial x_i} = \sum_{i=1}^{n} w_i \frac{\partial f_i(X)}{\partial x_i} + \sum_{j=1}^{k} \lambda_j \frac{\partial g_j(X)}{\partial x_i} = 0 \tag{5}$$

$$\frac{\partial L(X, \lambda, w)}{\partial \lambda_i} = g_j(X) = 0 \tag{6}$$

If a feasible solution X^* is the Pareto optimum of (1) and (2), then there exist multipliers $\lambda_j \ge 0$, $j = 1, ..., k$ and $w_i \ge 0$, $i = 1, ..., n$ satisfying,

$$\sum_{i=1}^{n} w_i \nabla f_i(X^*) + \sum_{j=1}^{k} \lambda_j \nabla g_j(X^*) = 0 \tag{7}$$

$$\lambda_j g_j(X^*) = 0, \quad j = 1, ..., k \tag{8}$$

These are necessary conditions for the Pareto optimum. They are also sufficient conditions for convex multiobjective problems when all objective functions and constraints are convex and $w_i > 0$.

3 Pareto-optimal solution

In general, no solution vector X exists that minimizes all n objective functions simultaneously. Hence, so-called Pareto-optimal solutions are sought in multiobjective optimization problems. A feasible solution X^* is called Pareto-optimal if there exists no other feasible solution X such that $f_i(X) \le f_i(X^*)$ for $i = 1, ..., n$. In other words, a feasible vector X^* is called Pareto optimal if there is no other feasible solution that would reduce some objective function without causing a simultaneous increase in at least one other objective function. In the global criterion method, the optimal solution X^* is found by minimizing a preselected global criterion $F(X)$, such as the sum of the squares of the relative deviations of the individual objective functions from the feasible solutions. Thus, X^* is formed by minimizing

$$F(X) = \sum_{i=1}^{n} \left(w_i \frac{f_i(X^*) - f_i(X)}{f_i(X^*)} \right)^p \tag{9}$$

$$\text{subject to } g_j(X) \le 0, \quad j = 1, ..., k \tag{10}$$

where p is a constant and X^* is the ideal solution for the objective function. The solution X^* is obtained by minimizing $f_i(X)$ subject to the constraints $g_j(X) \le 0$.

If the design variable vector has an infinitesimal perturbation in the neighborhood of optimization solution, the variations are assumed to be made along a prescribed projected directions so that the variation of the design variable vector is:

$$\delta X = \alpha S \tag{11}$$

The step length α along the search direction S can be given by:

$$\delta F(X) = \nabla F(X)^{\mathrm{T}} S \alpha \tag{12}$$

and the variation of the design variable vectors by:

$$\delta X = \frac{\delta F(X)}{\nabla F(X)^{\mathrm{T}} S} S \tag{13}$$

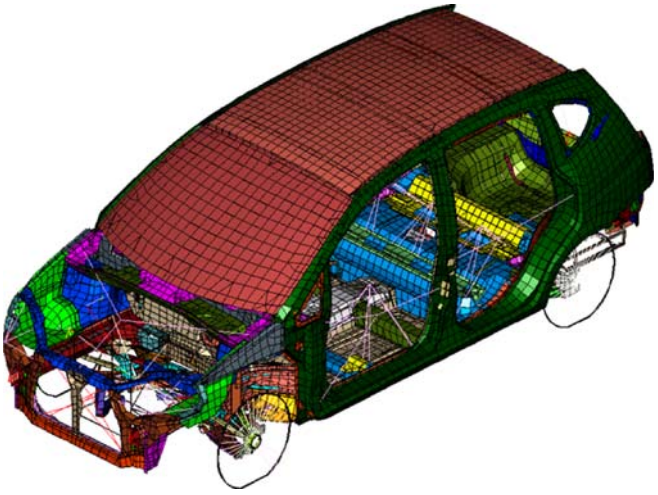

Fig. 1 Total vehicle model

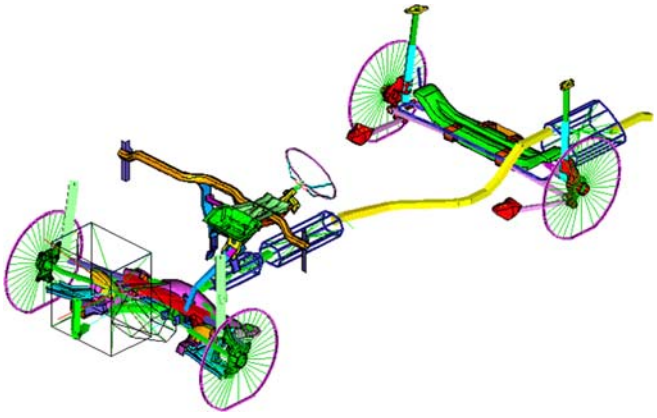

Fig. 2 Chassis system with suspension, exhaust, and steering systems

Using (12), the multiplication of (7) by S leads to:

$$\sum_{i=1}^{n} w_i \nabla f_i\left(X^*\right)^{\mathrm{T}} S + \sum_{j=1}^{k} \lambda_j \nabla g_j\left(X^*\right)^{\mathrm{T}} S = 0 \tag{14}$$

$$\sum_{i=1}^{n} w_i \nabla f_i\left(X^*\right)^{\mathrm{T}} S + \lambda^{\mathrm{T}} \nabla G^{\mathrm{T}} S = 0 \tag{15}$$

The direction-finding problem for obtaining a usable-feasible direction S can be formulated as:

$$\text{Find } S \text{ which minimizes } S^{\mathrm{T}} \nabla F(X) \tag{16}$$

$$\text{subject to } \nabla G^{\mathrm{T}} S = 0 \text{ and } S^{\mathrm{T}}\, S - 1 = 0 \tag{17}$$

From (16) and (17), we can derive the Lagrange function as

$$L(S, \lambda, \mu) = S^{\mathrm{T}} \nabla F(X) + \lambda^{\mathrm{T}} \nabla G^{\mathrm{T}} S + \mu\left(S^{\mathrm{T}} S - 1\right) \tag{18}$$

where $\lambda = \{\lambda_1 \lambda_2 ... \lambda_k\}^{\mathrm{T}}$. The Kuhn–Tucker optimality condition for the minimum is given by:

$$\frac{\partial L}{\partial S} = \nabla F(X) + \nabla G \lambda + 2\mu S = 0 \tag{19}$$

Table 1 Modal assurance criteria of updated vehicle model

Reference frequency range (TEST)	Verification frequency range (FEM)	MAC value (j=k)
24.47	24.38	0.95
25.76	26.22	0.93
29.77	30.03	0.85
32.75	32.98	0.86
37.65	38.42	0.88
39.47	40.02	0.83
42.45	43.18	0.84

FEM Finite element model, *MAC* modal assurance criteria

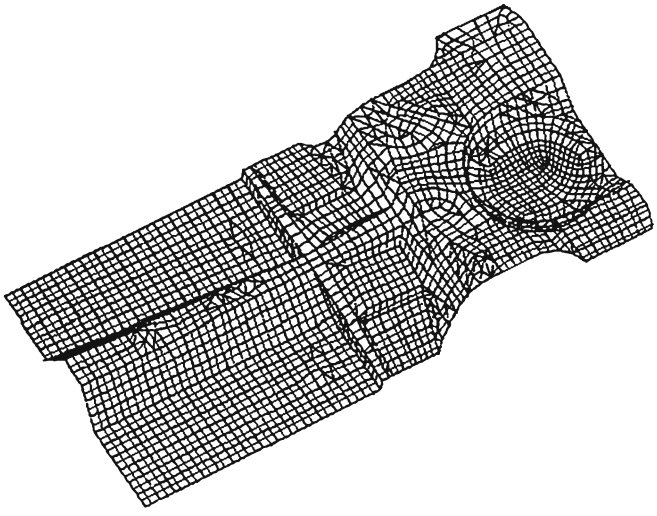

Fig. 3 Flat floor panel for topology optimization

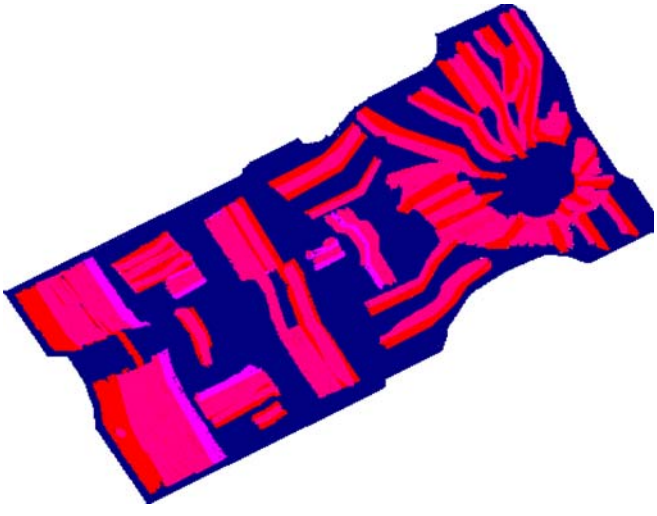

Fig. 4 Distribution of topological elements

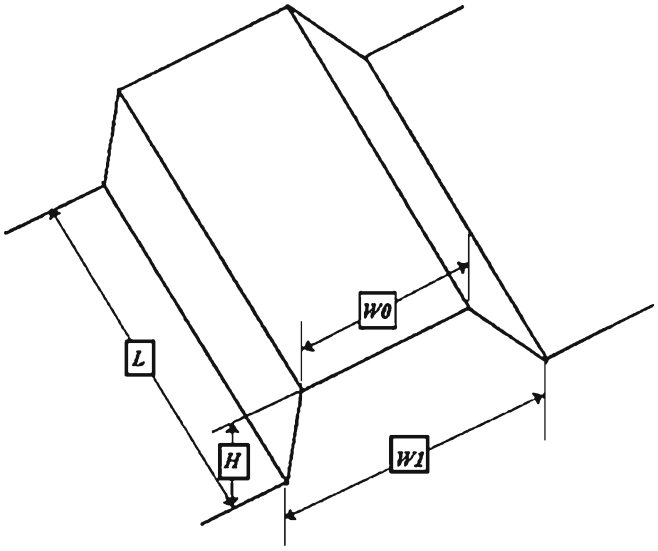

Fig. 5 Definitions of bead parameters

$$\frac{\partial L}{\partial \lambda} = \nabla G^{\mathrm{T}} S = 0 \tag{20}$$

$$\frac{\partial L}{\partial \mu} = S^{\mathrm{T}} S - 1 = 0 \tag{21}$$

Since $\nabla G^{\mathrm{T}} S = 0$, due to the orthogonality from Kuhn–Tucker optimality condition of a usable-feasible direction S, we have:

$$\sum_{i=1}^{n} w_i \nabla f_i\left(X^*\right) = 0 \tag{22}$$

For a Pareto-optimal solution, the condition of (22) can be satisfied in the feasible region.

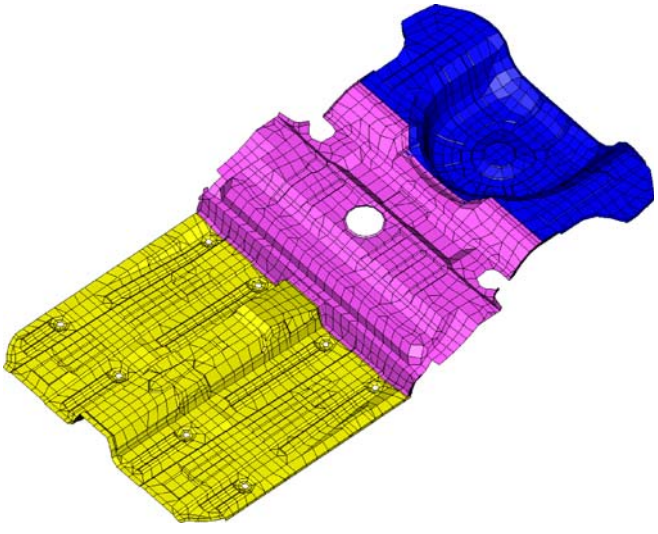

Fig. 6 Beaded floor panel

Table 2 Design variables in initial and optimization design

Design variables	Initial design	Optimized design
Dash cross member	1.50	0.85
Dash panel	0.85	0.70
Front rail BRKT at dash	1.40	1.15
Shock tower front UPR	2.35	1.75
Shock tower LWR	2.35	1.85
Fender support rail	0.80	0.80
Hinge pillar INR	0.80	0.85
Hinge pillar OTR	1.00	1.15
Front rail	1.20	1.25
Skirt	0.65	0.72
Steering column SPRT BRKT	1.60	1.65
Steering column SPRT BAR	2.00	2.00
Engine MTG bush stiffness, LH	171	139
Engine MTG bush stiffness, RH	125	115
Engine MTG bush stiffness, RR	140	130
Front floor panel	1.85	1.65
Rear floor panel	1.85	1.75

BRKT Braket, *UPR* upper, *LWR* lower, *INR* inner, *OTR* outer, *SPRT* support, *MTG* mounting, *LH* left handed side, *RH* right handed side, *RR* rear

4 Simulation

As an example, the dynamic characteristics of a vehicle model were simulated. Frequency is one of the most important factors influencing the overall noise, vibration, and harshness (NVH) quality of a passenger vehicle. In particular, the driver is sensitive to the vibrations of the steering wheel in the frequency range of engine idle shake, wheel shake, and road shake. By controlling these kinds of vibrations and understanding the current phenomena in more detail, a well-correlated finite element model can be found. Although deciding what the variables are is relatively simple, deciding how to apply them to a realistic model is a different problem in terms of feasibility and reliability. To obtain a reliable model, a total vehicle model with main components shown in Fig. 1 was validated with test results as shown in Table 1. The suspension, exhaust, and steering systems are shown in Fig. 2 as the chassis system attached to the body-in-white.

Table 3 Pareto-optimal solutions

Weighting			Body weight (kg)	Weighted average acceleration (m/s^2)
w_1	w_2	w_3		
0.05	0.90	0.05	1,460.1	0.37
0.10	0.80	0.10	1,463.8	0.32
0.15	0.70	0.15	1,469.3	0.21
0.20	0.60	0.20	1,471.3	0.16
0.25	0.50	0.25	1,474.4	0.15
0.35	0.325	0.325	1,480.5	0.12
0.40	0.30	0.30	1,480.5	0.12
0.50	0.25	0.25	1,480.5	0.15
0.60	0.20	0.20	1,395.2	0.21
0.70	0.15	0.15	1,386.4	0.29
0.80	0.10	0.10	1,380.7	0.31
0.90	0.05	0.05	1,374.5	0.44

The correlation between the test model and the finite element model was validated by modal assurance criteria (MAC) in (23). MAC values in the range of frequencies appear to be more than 80%, and this model is available for a feasible vehicle design study.

$$\mathrm{MAC}_{jk} = \frac{\left|\phi_{tj}^{\mathrm{T}}\phi_{ak}\right|^2}{\left(\phi_{ak}^{\mathrm{T}}\phi_{ak}\right)\left(\phi_{tj}^{\mathrm{T}}\phi_{tj}\right)} \tag{23}$$

This simulation modeled the vibration characteristics with respect to engine idle shake, wheel shake, and road shake. Engine excitation can be divided into two components: the unbalanced force due to the vertical force of the piston and the torque fluctuation due to pressure within the cylinders and the rotational moment.

For the unbalanced force, we have:

$$F = 4\left(m_{\mathrm{piston}} + m_{\mathrm{conrod}}\right)\frac{R^2\omega^2}{L^2}\cos 2\omega t \tag{24}$$

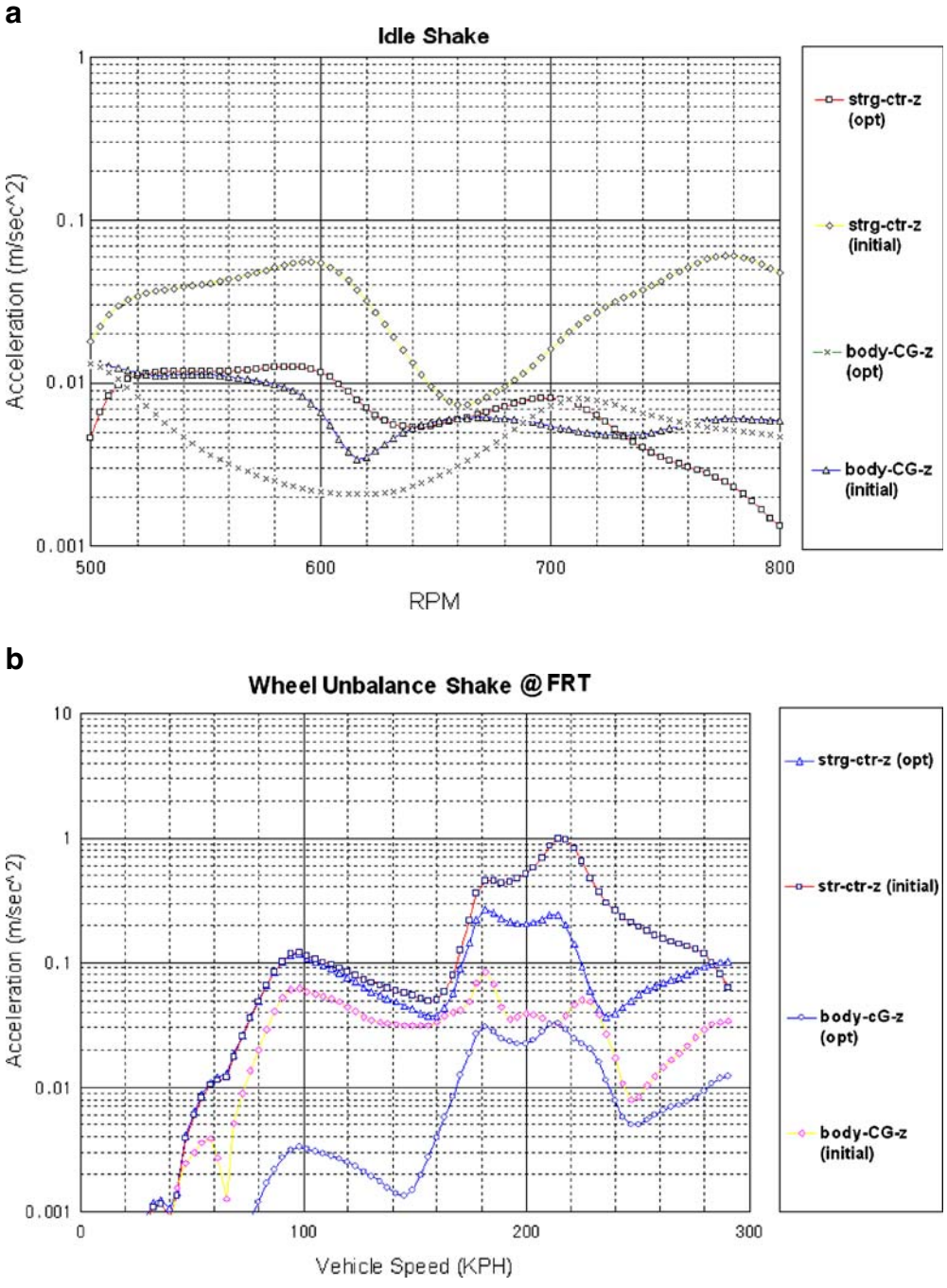

Fig. 7 Acceleration curve of steering wheel and body CG. **a** Under engine idle shake. **b** Under wheel shake. **c** Under road shake

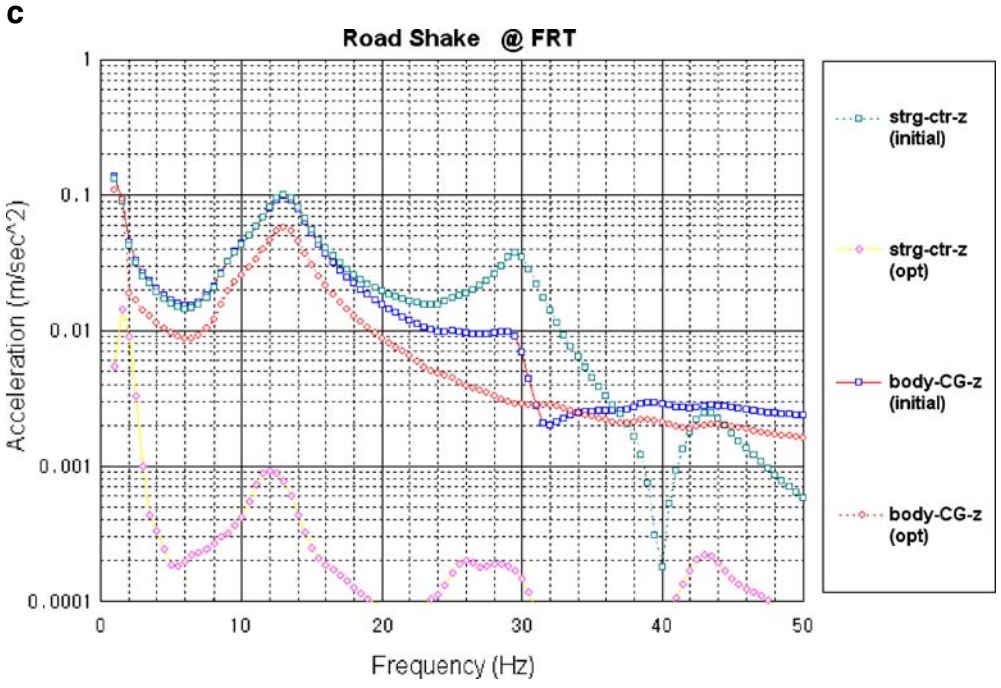

Fig. 7 (Continued)

For torque fluctuation, we have:

$$M = -2\left(m_{\text{piston}} + m_{\text{conrod}}\right)\omega^2 R^2 \sin 2\omega t \tag{25}$$

where m_{piston} and m_{conrod} are the piston mass and connecting rod mass, R is the crank radius, L is the connecting rod length, and ω is the angular velocity.

The excitations of wheel unbalance shake acted on the LH and RH front wheels with an unbalanced mass of 60 g:

$$F = Mr\omega^2 \tag{26}$$

where M is the unbalanced mass of the tire wheel, r is the radius of the wheel rim, and ω is the angular velocity of the wheel. Road shake is formulated as the excitation from the running road profile, which is a force amplitude applied at the hub vertically.

$$F = C/\text{freq}^n \tag{27}$$

where C and n are 353.84 and 0.7120543, respectively. They are correlated from the running test.

To analyze the dynamic stiffness of the vehicle body, sinusoidal forces were applied at the engine excitation point and the wheel rims. The accelerations of the steering wheel and body CG point were calculated in the frequency ranges and velocities specified in dynamic characteristics. The multicriteria optimization of panel thickness, average bush stiffness, and floor panel bead were performed for increasing dynamic stiffness. The damping ratio was set at 3% for the frequency range of interest. The optimization problem was to find the panel thickness, floor panel bead dimensions, and average bush stiffness that minimizes initial acceleration under a given frequency range, which includes the excitation by idle shake (f_{idle}), wheel shake (f_{wheel}), and road shake (f_{road}). The available design variables were 14 panel thicknesses, 13 beads, and 3 average bush stiffnesses.

$$\begin{aligned}\text{Minimize } F(X) &= w_1 f_{\text{idle}}(X) + w_2 f_{\text{wheel}}(X) \\ &\quad + w_3 f_{\text{road}}(X) \text{ for } \sum_{i=1}^{3} w_i = 1\end{aligned} \tag{28}$$

$$\begin{aligned}\text{subject to } & 0.8 \cdot (t_i)_0 \le t_i \le 1.2 \cdot (t_i)_0 \\ & 0.9 \cdot (k_{\text{bush }0})_j \le (k_{\text{bush}})_j \le 1.5 \cdot (k_{\text{bush }0})_j\end{aligned}$$

Beaded floor panels have been widely incorporated into automotive designs to improve dynamic stiffness (Wyckaert et al. 1997). The floor panel is designed to minimize its local deformation in the desired frequency range. Figure 3 depicts the initial floor panel model for topology optimization. Shape and sizing optimizations were simultaneously performed for the bead dimensions and panel thicknesses. Figure 4 shows the distribution of topological elements under vertical and twisting loads. The bead pattern can be defined parametrically in terms of length, width, and height. The thickness of the floor panel was included in the sizing optimization. Figure 5 shows bead parameters built on a flat floor: $W0$ and $W1$ are the bead's base and top width, respectively, and H and L are the bead's height and length, respectively. The height and width of the bead cannot be changed arbitrarily because of manufacturing limitations. After carefully considering the involved factors, a cross-section must be chosen. The lengths

of beads are prechosen in the topology optimization. The geometrical constraints of bead parameters are as follows:

$$\begin{aligned} \text{For each bead,} \quad h^L &\le \text{change of height } (h) \le h^u \\ w^L &\le \text{change of width } (w) \le w^u \\ a_j^L &\le \text{configuration vector } (a_j) \le a_j^u,\ j = 1...n \end{aligned}$$

where h and w are the dimensions of the reinforced bead in the inner panel, and a_j is the move vector of the bead shape.

Figure 6 shows the beaded floor panel made through multicriteria optimization. Table 2 shows the design variables of the initial and optimized designs. Table 3 shows the Pareto-optimal solutions obtained by weighting the design factors. Figure 7 shows the acceleration at the steering center and the body CG. The optimized design shows marked improvement in acceleration over the baseline model.

5 Conclusions

The optimization design methodology was explained using automotive body design for securing structural rigidities of a panel-made structure using a lightweight design. For the reinforcement of the geometric dimensions of the panel structure, the topological distributions of structural reinforcement were determined by topology optimization, and more detailed dimensions, such as panel thickness and mounting location, were designed by shape and sizing optimization. The most feasible designs can be made through the integration of multicriteria optimization and Pareto-optimal sensitivity for various performance parameters and constraints. This analytical procedure provides an efficient design for many mechanical structures in the early stages of their development.

Acknowledgements This work is financially supported by the Ministry of Education and Human Resources Development (MOE), the Ministry of Commerce, Industry and Energy (MOCIE) and the Ministry of Labor (MOLAB) through the fostering project of the Lab of Excellency.

References

Bendsoe MP (1989) Optimal shape design as a material distribution problem. Struct Optim 1:193–202

Bendsoe MP, Kikuchi N (1988) Generating optimal topologies for structural design using a homogenization method. Comput Methods Appl Mech Eng 71:197–224

Bendsoe MP, Guedes JM, Haber RB, Pedersen P, Taylor JE (1994) Analytical model to predict optimal material properties in the context of optimal structural design. J Appl Mech 61(4):930–937

Devaraj SR, Kridli GT, Shulze RC (2005) Design and analysis of a conceptual modular aluminum spaceframe platform. In: SAE 2005-01-1029

Ding YL (1986) Shape optimization of structures: a literature survey. Comput Struct 24(6):985–1004

Heo JH, Ehmann KF (1991) A method for substructural sensitivity synthesis. J Vib Acoust 113:201–208

Huizinga ATMJM, Campen DH, Kraker A (1997) Application of hybrid frequency domain substructuring for modeling and automotive engine suspension. J Vib Acoust 119:304–310

Lee D-C (2004) A design of panel structure for the improvement of dynamic stiffness. Proc Int Mech Eng D J Automot Eng 218(6):647–654

Lee D-C, Lee J-I (2003) A structural optimization design for aluminum-intensive vehicle. Proc Int Mech Eng D J Automot Eng 217(9):771–779

Nakagawa T et al (2004) First-order analysis for automotive body structure design-part 4: noise and vibration analysis applied to a subframe. In: SAE 2004-01-1661

Nishigaki H, Kikuchi N (2004) First-order analysis for automotive body structure design—part 3: crashworthiness analysis using beam elements. In: SAE 2004-01-1660

Raasch I (2004) Sizing in conceptual design at BMW. In: SAE 2004-01-1657

Rao SS (1996) Engineering optimization-theory and practice, 3rd edn. Wiley, New York

Tsurumi Y et al (2004) First-order analysis for automotive body structure design-part 2: joint analysis considering nonlinear behavior. In: SAE 2004-01-1659

Wyckaert K, Brughmans M, Zhang C, Dupont R (1997) Hybrid substructuring for vibro-acoustical optimisation: application to suspension—car body interaction. In: Proceedings of the SAE noise and vibration conference. pp 591–598